American Mineralogist, Volume 68, pages 494–505, 1983

Lindsleyite (Ba) and mathiasite (K): two new chromium-titanates in the crichtonite series from the upper mantle

STEPHEN E. HAGGERTY

Department of Geology
University of Massachusetts, Amherst, Massachusetts 01003

J. R. SMYTH[1]

Los Alamos Scientific Laboratory
Los Alamos, New Mexico

A. J. ERLANK, R. S. RICKARD

Department of Geochemistry
University of Cape Town, Republic of South Africa

AND R. V. DANCHIN[2]

Anglo-American Corporation Research Laboratory
Crown Mines, Johannesburg, Republic of South Africa

Abstract

Two new opaque minerals are described from metasomatized peridotites and heavy media concentrates from four kimberlites in the Republic of South Africa. Lindsleyite and mathiasite are the Ba and K members of the $AM_{21}O_{38}$ series, characterized by predominant A-specific, *large* cations (Sr = crichtonite; Na = landauite; Pb = senaite; Ca = loveringite, and U + REE = davidite), and by M-formula *small* cations which are dominantly Ti, Cr, Fe, Mg, Zr, and Nb. Approximately 70% of the A-site is filled by either Ba or K in the new minerals, and selective solid solution is present with Ba–Sr and K–Ca exchange. Typical electron microbeam analyses based on 38 oxygens, give the following formulae:

lindsleyite: A = $Ba_{0.62}Sr_{0.41}Ca_{0.09}Pb_{0.01}K_{0.07}Na_{0.06}REE_{0.03}$
M = $Ti_{11.63}Zr_{0.87}Al_{0.11}Cr_{3.89}Fe_{2.87}Mg_{1.49}Nb_{0.08}$
mathiasite: A = $K_{0.66}Ca_{0.22}Sr_{0.15}Ba_{0.10}Na_{0.05}REE_{0.05}$
M = $Ti_{13.18}Zr_{0.62}Cr_{2.87}Fe_{2.28}Mg_{1.63}Ca_{0.22}Nb_{0.09}$

REE in both minerals share the unusual characteristic of davidite and loveringite in possessing LREE- and HREE-enrichment, with depletion of the middle lanthanides.

The space group for both minerals is $R3$ or $R\bar{3}$ and the strongest reflections are 2.13, 1.80, 1.59, and 1.44Å (all 100) for lindsleyite, and 2.25(90), 2.14 (100), and 1.44 Å (100) for mathiasite. Hexagonal unit cell parameters for lindsleyite are a = 1.037 nm, c = 2.052 nm, V = 1.911 nm^3, and for mathiasite are a = 1.035 nm, c = 2.058 nm, V = 1.909 nm^3. Calculated densities for the Ba and K members are 4.63 and 4.60 gm/cm^3, respectively.

Both minerals are black and have a metallic luster and conchoidal fracture. The minerals are pale tan in reflected light, exhibit weak reflection pleochroism and weak-moderate reflection anisotropy. Spectral reflectances for lindsleyite and mathiasite are very similar and are comparable to ilmenite and rutile. R_1 and R_2 in air and oil, respectively, for lindsleyite are: 470 nm = 17.9–18.3%, 5.9–6.1%; 546 nm = 17.0–17.3%; 5.3–5.5%; 589 nm = 16.7–17.0%, 5.1–5.3%; 650 nm = 16.5–16.9%, 5.0–5.2%. Similar data for mathiasite are:

[1] Present address: Department of Geology, University of Colorado, Boulder, Colorado 80309.
[2] Present address: Stockdale Prospecting Ltd., 60 Wilson Street, South Yarra, Victoria 3141, Australia.

0003–004X/83/0506–0494$02.00

470 nm = 18.3–19.0%, 5.9–6.4%; 546 nm = 17.1–17.9%, 5.3–5.8%; 589 nm = 16.7–17.5%, 5.1–5.6%; 650 nm = 16.5–17.3%, 5.0–5.5%. The mean Vickers microhardness value for mathiasite is 1505 Kg/mm^2; lindsleyite is judged to be comparable.

Associated characteristic minerals are K-richterite, phlogopite, Nb-Cr-rutile and Nb-Cr-Mg-ilmenite, together with olivine, orthopyroxene, Cr-diopside, and Mg-Cr-spinel. Garnet is typically absent. The new minerals formed by metasomatizing fluids enriched in K + Ba + REE + Ti that infiltrated source rocks depleted in Al and contaminated perhaps by Cr prior to the eruption of kimberlite, providing important potential insights to the dynamics of fluid movements, and the compositions of fluids in the upper mantle.

Lindsleyite is named in honor of Professor Donald H. Lindsley, and mathiasite in honor of Professor Morna Mathias, for their respective contributions to experimental mineralogy and the petrology of alkalic suites. The minerals and the names have been approved by the Commission on New Minerals and Mineral Names of the I.M.A.

Introduction

The crichtonite mineral series is defined as having a principal large cation, Sr(crichtonite), Pb(senaite), U-REE(davidite), Na(landauite), and Ca(loveringite) occupying the A position in $AM_{21}O_{38}$ (Grey *et al.*, 1976; Grey and Lloyd, 1976; Gatehouse *et al.*, 1978; Grey and Gatehouse, 1978). In lindsleyite and mathiasite, the two new minerals described here, the large cation position is dominantly Ba and K, respectively. The small cations(M) in the isomorphous series are Fe, Mg, Mn, Zn, Cr, Al, Ti, and Zr. Apart from the large cations, the new minerals may be compositionally classified as Fe–Zr–Mg chromian titanates.

Lindsleyite was originally identified by Haggerty (1975) from the De Beers kimberlite in the Republic of South Africa (RSA) and the mineral has since been recognized by Erlank and Rickard (1977), Smyth *et al.* (1978), and Jones *et al.* (1982) as an accessory mineral in veined peridotites from nearby Bultfontein. Mathiasite, the K member has thus far been recognized in heavy mineral concentrates from the Jagersfontein mine, the Kolonkwanen kimberlite, and in one veined peridotite from Bultfontein, all in the RSA. There is evidence for some degree of solubility between lindsleyite and mathiasite, and although the precise conditions of formation remain speculative, these minerals share a number of common features demonstrating a genetic link. The most convincing is that *both* phases are present as discrete crystals in a single veinlet in peridotite. Characteristic minerals associated with both mathiasite and lindsleyite are phlogopite, diopside, K-richterite, Nb–Cr-rutile, and Mg–Cr–Nb-ilmenite. All indications are that these phases formed in the upper mantle.

Lindsleyite is named in honor of Professor Donald H. Lindsley, of the Department of Earth and Space Sciences, State University of New York at Stony Brook, in recognition of his contributions to mineralogy, to the development of the benchmark, Fe–Ti oxide geothermometer–oxygen geobarometer, and to his high pressure phase equilibria studies in oxide and silicate systems.

Mathiasite is named in honor of Professor Morna Mathias, formerly of the Department of Geology, University of Cape Town, in recognition of her foundation studies on alkaline rocks, and to her early contribution on the mineralogy, petrology, and geochemistry of mantle-derived eclogites and peridotites.

Lindsleyite and mathiasite have been approved by the Commission on New Minerals and Mineral Names of the International Mineralogical Association. Type materials are deposited at the Smithsonian Institution, Washington, D.C., the South African National Museum, Cape Town, and the British Museum (Natural History) London.

Sample locations and descriptions

The Kimberley district in the Republic of South Africa is world renowned for its high productivity in diamonds that have been actively mined for the past century. Lindsleyite is recognized at the De Beers mine and thus far only one grain, 1.5 mm in longest dimension, has been identified, mantled by perovskite and enclosed in a subhedral grain of low titanium phlogopite, embedded in kimberlite. The mineral is also present at Bultfontein in peridotite samples derived from processed kimberlite that was spread out on "floors" and disaggregated by steam rolling in the early days of mining. These "floors" contain vast quantities of resistent nodules that have been the subject of numerous studies detailed by Ahrens *et al.* (1975) and Boyd and Meyer (1979a,b). In some nodules, lindsleyite grains up to 3 mm in dimension are present in K-richterite and phlogopite-rich (Fig. 1a) anastomosing metasomatized veinlets 2–3 cm wide, penetrating nodules of rounded peridotite. In other nodules that are not veined the mineral occurs as irregular polycrystalline masses, often completely enclosed within Cr-diopside grains (Fig. 1b). Individual crystal sizes range up to 5 mm and aggregates of these are partially rimmed by rutile that contain minor inclusions of ilmenite or Cr-rich spinel. Fifteen lindsleyite-bearing nodules have so far been recognized by us and Jones *et al.* (1982).

Jagersfontein is ≈130 km SE of Kimberley in the Orange Free State. The mine is no longer active, but the nodule suite from this kimberlite, in common with that

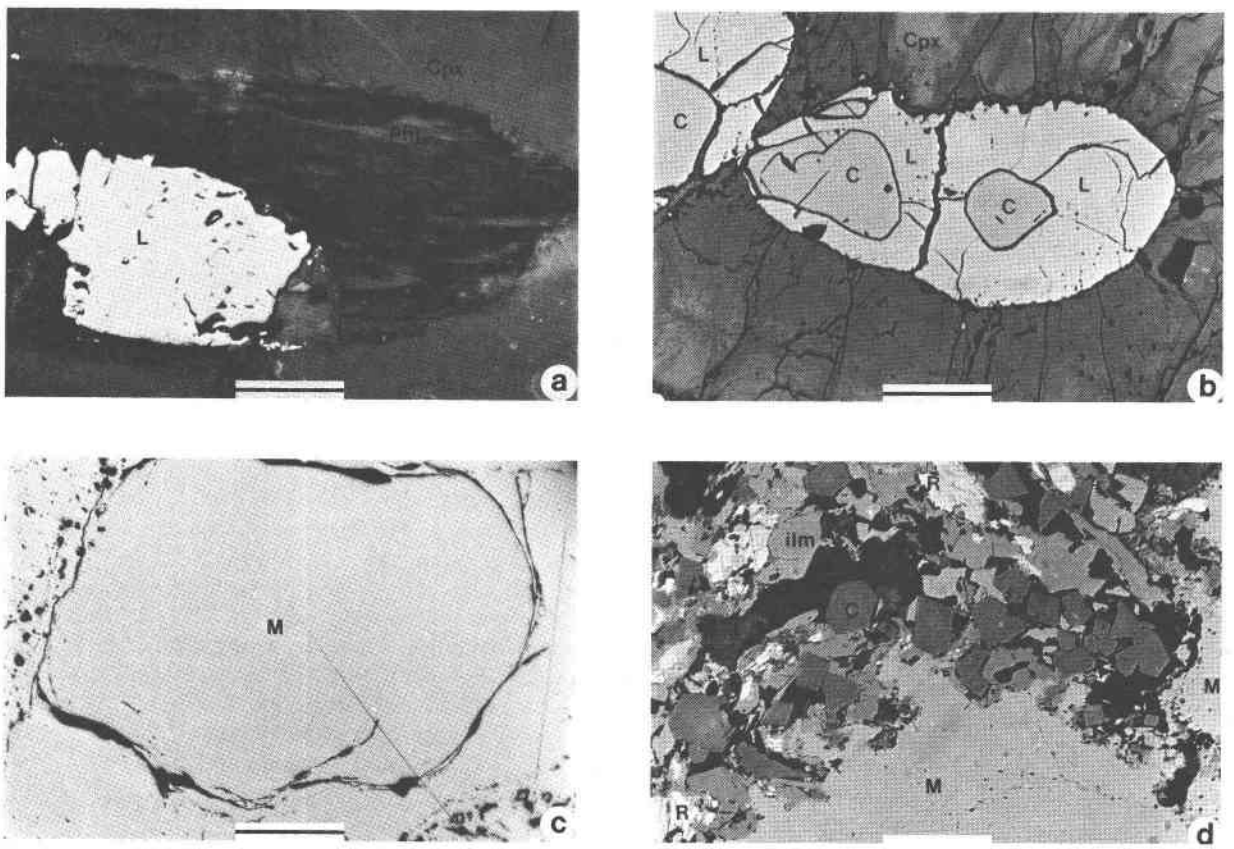

Fig. 1. (a) Lindsleyite (L) enclosed in phlogopite (Phl) and surrounded by chrome diopside (Cpx) and K-richterite (Ric). Sample BD-3096, Bultfontein. Mixed reflected and transmitted light in oil-immersion. Scale bar = 0.1mm. (b) Lindsleyite (L) enclosing chrome spinel (C) and surrounded by chrome diopside (Cpx). Sample JJG-360, Bultfontein. Reflected light in air. Scale bar = 0.2mm. (c) Mathiasite (M) exhibiting typical curvilinear cracks and incipient decomposition (upper left and lower right). Sample JF18-1, Jagersfontein. Reflected light in air. Scale bar = 0.2mm. (d) Mathiasite (M) decomposing to chrome spinel (C) + ilmenite (ilm) + rutile (R). The rutile contains oriented sigmoidal lamellae of ilmenite and the dark interstitial groundmass is composed of phlogopite (Phl), calcite, and sphene. Sample JF-111, Jagersfontein. Reflected light in oil-immersion. Scale bar = 0.1mm.

from Bultfontein, has received considerable attention over the past decade in characterization studies of the mantle underlying these regions (*e.g.*, MacGregor and Carter, 1970; Johnston, 1973; Harte and Gurney, 1982). A number of exotic phases and assemblages are present, and these include armalcolite, first recognized in lunar samples, Nb–Cr rutile which is more typical of alkalic rocks (Haggerty 1982; submitted), diamond in graphite, and spinel-to-garnet transition lherzolites (Haggerty, 1979). Mathiasite, or more correctly, members of the K–Ba–Ca series were recovered from heavy mineral concentrates at Jagersfontein but recognized only in polished section along with ilmenite, Cr-spinel, and Nb–Cr-rutile. Massive, homogeneous and polycrystalline aggregates range from 0.5 to 5 cm and many of these appear to be single crystals, sub-spherical in shape with dimpled surfaces and an outer matte luster. Twenty-nine macrocrysts have so far been recognized from a suite of 365 hand-picked opaque mineral grains. Their compositions have been characterized and associated minerals include olivine, diopside, phlogopite, Ce-bearing barites, Nb–Cr-rutile, Mg–Cr-spinel and ilmenite, perovskite or sphene, and an unidentified Zr-silicate (Haggerty, submitted).

Kolonkwanen, in the Mackenzie's Post district of the northern Cape Province, is located close to the border with Botswana. It is a non-diamondiferous kimberlite prospect and, little is known of its mineralogy or chemistry. In exploration and evaluation of the kimberlite, mathiasite was recognized by one of us (RVD) as the dominant opaque phase present in heavy mineral concentrates. In most respects the mathiasite from Kolonkwanen is similar to the material from Jagersfontein.

Finally, it is noteworthy that lindsleyite and mathiasite occur together in the same K-richterite and phlogopite-rich vein in a peridotite from the Bultfontein "floors" (sample BD3096). It is likely that this will also prove to be the case for other Bultfontein nodules we have qualitatively studied thus far.

Optical and physical properties

Lindsleyite and mathiasite are opaque minerals, black in color, with a conchoidal fracture, and a metallic luster, bearing a close macroscopic resemblance to ilmenite and rutile. In reflected light the minerals are opaque, even at very thin edges and no internal reflections are observed. Lindsleyite is tan, weakly pleochroic in shades of buff-white to tan, and exhibits weak reflection pleochroism from pale tan to brown. Mathiasite is a darker tan, also weakly pleochroic but more strongly anisotropic in shades of tan brown to darker brown. Lindsleyite has a slightly lower reflectivity than mathiasite, but the spectral reflectances between 400 and 700 nm decrease progressively along very similar paths (Table 1). These data were obtained using a method similar to that described by Criddle (Cabri *et al.*, 1981) and undertaken by C. J. Stanley of the British Museum (Natural History).

Relative to other associated opaque minerals, lindsleyite and mathiasite are similar in color and reflectivity to ilmenite and rutile. The new minerals are distinguished from ilmenite by their paler tan color, and weaker anisotropy and reflection pleochroism, and by characteristic curvilinear fracture patterns (Fig. 1c). In contrast to rutile, the new minerals are tan rather than gray-white, have lower reflectivities, and lack internal reflections or twinning characteristics. Mathiasite and lindsleyite are distinctly lighter in color and have higher reflectivities in comparison to the typically subdued gray tones and lower reflective properties of Cr-Mg-spinel, and armalcolite.

Other optically distinguishing features are in the breakdown products which are rutile + spinel±ilmenite, intimately associated with sphene or perovskite + calcite. This assemblage is present in spherical, triangular-shaped pools at the triple junctions to curvilinear fractures (Fig. 1d). Another useful property is the absence of sigmoidal lenses of ilmenite which are so commonly present in kimberlitic rutiles.

The calculated densities for lindsleyite and mathiasite are 4.63 and 4.60 gm/cm^3, respectively. The range in Vickers microhardness for mathiasite is 1378–1714 kg/mm^2 (14 determinations) with a mean of 1505 kg/mm^2, under a 100 gram force, for an indentation duration of 15 sec, measured in green light at ≈546 nm (Criddle, 1980). Indentations are either perfect or slightly fractured in radial patterns. Because of the similarities in major element chemistry, structure, and other physical properties, it is estimated that lindsleyite (currently observed only in polished-thin sections) has a comparable hardness to that of mathiasite.

Table 1. Quantitative reflectance data

	Lindsleyite				Mathiasite			
	air		oil		air		oil	
nm	R_1%	R_2%	R_1%	R_2%	R_1%	R_2%	R_1%	R_2%
400	19.4	19.8	6.7	7.1	20.1	20.8	6.9	7.5
420	19.0	19.2	6.5	6.8	19.5	20.2	6.6	7.1
440	18.6	18.9	6.3	6.5	19.0	19.7	6.3	6.8
460	18.1	18.4	6.0	6.2	18.5	19.2	6.1	6.5
480	17.8	18.1	5.8	6.0	18.1	18.8	5.8	6.3
500	17.5	17.8	5.6	5.8	17.7	18.4	5.6	6.1
520	17.2	17.5	5.4	5.6	17.4	18.2	5.5	6.0
540	17.1	17.3	5.3	5.5	17.2	17.9	5.3	5.8
560	16.9	17.1	5.2	5.4	16.9	17.7	5.2	5.7
580	16.7	17.0	5.1	5.3	16.8	17.6	5.1	5.6
600	16.7	16.9	5.1	5.3	16.6	17.4	5.1	5.6
620	16.6	16.9	5.1	5.3	16.5	17.4	5.0	5.5
640	16.5	16.8	5.0	5.2	16.5	17.3	5.0	5.5
660	16.5	16.9	5.0	5.2	16.5	17.3	5.0	5.5
680	16.5	16.9	5.1	5.2	16.4	17.3	5.0	5.5
700	16.5	16.9	5.1	5.3	16.4	17.3	5.0	5.5

Lindsleyite: sample 75933 - De Beers. Mathiasite: sample JAG80-26(4) - Jagersfontein.

Data obtained from single unoriented grains at extinction positions using: Zeiss x16 objectives, effective NA 0.2, plane glass reflector, SiC No. 472, and a Hammamatsu R928 photocathode. Immersion measurements made using Zeiss oil N_D1.515, DIN 58.884.

Mineral chemistry

Methods of analysis

Lindsleyite and mathiasite were analyzed using electron microbeam techniques. Different samples of both minerals were analyzed at the University of Cape Town on a Cambridge Microscan 5 instrument, at Los Alamos on a Camebex model Cameca microprobe, and at the University of Massachusetts on a ETEC Autoprobe. The original lindsleyite was analyzed on a MAC probe at the Geophysical Laboratory, Carnegie Institution of Washington. Standards used in these investigations were natural (N) minerals, synthetic (S) compounds, or glasses (G). The following list (U.Mass.) is typical of those used in this collaborative investigation: Banana ($Ba_2NaNb_5O_{15}$)–S for Ba, Na, Nb; or single crystal pyrochlore—N for Na, Nb, Ta, Zr; or ZrO_2—S for Zr; Ba, celsian-S or Banana; sanidine-N for K; Cr, Mg, and Ti, armalcolite-S; Cr, Mg, and Al, 52NL11 (chromite)—N; Fe, Mn, and Ti, Mn-ilmenite—N; Sr and Ti, $SrTiO_3$—S; Ta and K, $KTaO_3$—S; Pb, Corning 24—G or $PbBr_2$-S. REE glasses (Drake and Weill, 1972) were also used for Ca and Si and LREE also employed natural pyrochlore and Wilberforce apatite. Operating voltages were either at 15 or 20 kV, sample currents of either 0.02 or 0.03 μA and counting times of 15–50 sec. The correction procedures employed were either those of Bence and Albee (1968), and Albee and Ray (1970) or the ZAF method. Particular attention was given to overlapping peak positions for Ba and Ti, Ti and V, and interferences among the REE. Second order corrections were applied to REE analyses following the approach by Åmli and Griffin (1975) and these have resulted in reproducible analyses of the standards, of lindsleyite and mathiasite. The worst possible case (*i.e.*, maximum corrections) is applied to the data presented in this paper.

Our analyses of lindsleyite and mathiasite are presented in Table 2 along with data reported by Jones *et al.* (1982) for the former. A comparison of these minerals with other members of the $AM_{21}O_{38}$ series are also listed. Calculated cation concentrations based on 38 oxygens are given in Table 3.

Table 2. Compositions of minerals in the $AM_{21}O_{38}$ series

	Lindsleyite									Mathiasite									Loveringite		Chrich-tonite	Sena-ite	David-ite	Landau-ite
	75933			BD3096	JJG	JJG	JJG	H-1				BD3096	JF	JF	JF	"LIMA"								
	Range	Av	Rep	(1)	360(1)	360(2)	360(3)	Av	Range	BD-2	BD-4	(2)	26-3	41-1	50-1	Av	Range		Av	Range				
SiO_2	0.00	0.00	0.00	--	--	--	--	0.01	0.00-0.04	--	--	--	0.00	0.00	0.00	0.00	0.01		0.20	0.07-1.38	--		--	--
TiO_2	53.91-54.58	54.28	54.36	57.06	52.7	58.4	57.2	59.64	57.20-63.00	60.8	59.9	59.61	60.23	61.55	59.23	59.32	58.13-60.78		58.06	54.67-64.10	60.49	58.68	51.74	72.59
V_2O_5	1.91-0.62	0.98	0.69	--	--	--	0.76	--	-- --	--	--	--	--	--	--	--	-- --		1.30	0.37-4.40	0.61	0.70	2.88	--
ZrO_2	3.99-4.06	4.02	4.06	2.42	6.1	2.9	4.38	3.41	2.32-4.93	4.4	5.1	2.60	4.73	4.48	4.62	5.35	3.97-7.06		4.38	1.21-6.12	0.10	0.09	0.07	0.30
HfO_2	-- --	--	--	--	--	--	--	--	-- --	--	--	--	--	--	--	--	-- --		0.21	0.03-0.35	0.23	0.13	0.51	--
Al_2O_3	0.07-0.14	0.09	0.14	0.29	--	--	--	0.59	0.11-1.22	--	--	0.17	0.59	0.55	0.63	0.62	0.50-0.83		0.96	0.58-1.54	0.02	0.05	0.22	--
Cr_2O_3	16.19-16.27	16.22	16.21	12.64	16.8	15.1	16.24	15.10	14.20-17.50	12.6	13.0	12.43	16.42	16.32	17.02	16.71	15.79-18.06		5.97	0.06-9.94	0.15	0.16	1.21	--
Fe_2O_3	-- --	--	--	--	13.0	11.0	11.33	--	-- --	10.5	10.4	--	--	--	--	--	-- --		20.01	15.77-26.76	21.14	16.20	25.30	6.77
FeO	11.04-11.42	11.20	11.42	13.31	--	--	--	11.22	7.37-13.40	--	--	13.03	8.29	6.68	8.24	7.96	6.78-8.71		--	-- --	8.18	8.53	--	1.26
MgO	3.46-3.60	3.54	3.60	3.19	3.4	3.7	3.30	3.32	2.88-3.88	3.8	3.6	3.05	4.14	4.22	4.13	4.12	3.82-4.30		1.38	0.63-2.18	--	0.02	0.10	--
MnO	0.15-0.25	0.19	0.25	--	--	--	0.15	0.08	0.00-0.11	--	--	--	0.15	0.19	0.17	0.14	0.01-0.24		0.15	0.03-0.21	2.78	4.08	0.04	4.12
CaO	0.37-0.49	0.42	0.37	0.26	0.3	0.5	0.34	0.80	0.22-1.69	0.7	0.7	0.52	1.27	0.80	1.03	1.09	0.76-1.36		2.50	1.45-4.54	0.06	0.10	0.23	--
ZnO	-- --	--	--	--	--	--	--	--	-- --	--	--	--	--	--	--	--	-- --		--	-- --	--	--	--	10.85
SrO	1.47-1.95	1.69	1.95	1.10	2.4	1.5	2.36	1.18	0.47-1.60	0.9	0.9	1.10	--	0.78	0.78	0.66	0.00-1.62		0.01	0.01-0.01	4.17	0.20	0.02	--
BaO	4.58-4.64	4.60	4.64	5.65	5.4	3.1	2.09	2.56	0.35-5.39	0.9	0.8	1.77	1.17	1.00	0.81	0.96	0.33-3.19		--	-- --	--	--	--	--
PbO	0.05-0.10	0.07	0.10	--	--	--	--	--	-- --	--	--	--	--	0.02	--	0.02	0.00-0.09		0.08	0.05-0.23	0.78	9.21	0.69	2.10
Na_2O	0.01	0.01	0.01	--	--	--	0.11	0.10	0.04-0.18	0.1	--	--	0.10	0.09	0.02	0.09	0.03-0.18		0.04	0.06-0.13	--	--	--	1.36
K_2O	0.19-0.23	0.21	0.19	0.18	0.2	0.5	0.30	0.55	0.17-0.81	1.8	1.8	1.18	1.25	0.97	1.17	1.22	0.91-1.38		0.04	0.04-0.04	--	--	--	0.45
Nb_2O_5	0.00-0.07	0.02	0.00	0.76	0.6	0.6	1.06	0.02		0.7	0.7	0.87	0.03	0.00	0.00	0.15	0.00-0.94		--	-- --	--	--	--	0.29
Ta_2O_5	0.02-0.04	0.03	0.02	--								--	0.00	0.00	0.19	0.08	0.00-0.47		--	-- --	--	--	--	
Y_2O_3	0.01	0.00	0.00	--								--	0.00	0.00	0.00	0.01	0.00-0.03		0.18	0.09-0.27	0.21	0.86	1.86	--
La_2O_3	0.01-0.08	0.05	0.08	0.18								0.34	0.00	0.33	0.06	0.19	0.08-0.54		1.23	0.08-2.43	0.29	0.06	3.35	--
Ce_2O_3	1.27-1.41	1.36	1.41										0.17	0.61	0.53	0.35	0.05-0.60		1.12	-- --	0.27	0.07	3.06	--
Pr_2O_3	-- --	--	--										--	--	--	0.00	0.00-0.00		--	-- --	--	--	--	--
Nd_2O_3	0.00-0.02	0.01	0.02										0.06	0.08	0.00	0.07	0.00-0.17		0.26	0.05-0.35	0.02	0.01	0.35	--
Sm_2O_3	0.01	0.00	0.00										0.00	0.00	--	0.01	0.01							
Eu_2O_3	0.06-0.10	0.08	0.10										0.00	0.00	0.00	0.01	0.00-0.04							
Gd_2O_3	0.01	0.00	0.00										0.00	0.00	0.00	0.01	0.01							
Tb_2O_3	0.00-0.10	0.04	0.00										0.00	0.00	0.24	0.03	0.00-0.13							
Dy_2O_3	0.01	0.00	0.00										0.00	0.00	--	0.01	0.01							
Ho_2O_3	0.00-0.07	0.03	0.00										0.00	0.00	--	0.04	0.00-0.12							
Er_2O_3	0.14-0.42	0.27	0.41										0.14	0.28	--	0.21	0.00-0.34							
Tm_2O_3	0.10-0.21	0.19	0.18										0.15	0.06	0.15	0.39	0.01-0.79							
Yb_2O_3	0.01	0.00	0.00										0.00	0.00	--	0.01	0.01							
Lu_2O_3	0.11-0.21	0.18	0.16										0.14	0.17	0.13	0.67	0.00-1.34							
RE_2O_3													--	--	--	--	-- --		0.45	0.03-0.30	--	--	0.88	
U_3O_8	0.01	0.00	0.00										0.00	--	--	0.01	0.01		0.14	0.17-0.34	--	--	6.42	
ThO_2	0.01	0.00	0.00										0.00	--	--	0.01	0.01		0.27	0.09-0.53	0.01	0.12	0.05	
TOTAL		99.78	100.37	97.04	100.9	97.3	99.62	98.58		97.2	96.9	96.67	99.03	99.18	99.15	100.46					99.51	99.35	98.98	100.09
Column #	1 2	3	4	5	6	7	8	9	10 11	12	13	14	15	16	17	18	19 20		21	22 23	24	25	26	27

Lindsleyite: 75933 DeBeers Reanalyses of original grain (Haggerty, 1975); BD3096(1), JJG 360 and H-1 are from the Bultfontein "Floors." H-1 is from Jones et al. (1982).

Mathiasite: BD-2 and BD-4 Kolonkwanen; BD3096(2) Bultfontein; JF 26-3, JF 41-1, and JF 50-1 Jagersfontein; "LIMA" refers to lindsleyite-mathiasite (with loveringite in solid solution) reported for 29 nodules from Jagersfontein (Haggerty, 1983, submitted).

Analysts: Columns 1-4 and 15-20 Haggerty; Columns 5, 7 and 15 Erlank and Rickard; Columns 6 and 8 and 12-13 Smyth.

Loveringite: Campbell and Kelly (1978); Crichtonite (Grey et al., 1976); Davidite (Gatehouse et al., 1978); Landauite (Grey and Gatehouse, 1978). Senaite (Grey et al., 1976) also contains 0.08 NiO.

Table 3. Formulae of crichtonite series minerals

		Sum large cations		Sum small cations	Cation Totals
		LINDSLEYITE			
De Beers 75933					
Average:	$(Ba_{.55}K_{.08}Na_{.007}Pb_{.11}Sr_{.30}Ca_{.14}REE_{.25})$	A=1.437	$(Ti_{12.36}Zr_{.59}V_{.2}Al_{.03}Cr_{3.88}Fe_{2.84}Mg_{1.60}Mn_{.05}Nb_{.004}Ta_{.004})$	M=21.558	22.995
Representative:	$(Ba_{.55}K_{.07}Na_{.006}Pb_{.008}Sr_{.34}Ca_{.12}REE_{.25})$	A=1.344	$(Ti_{12.34}Zr_{.6}V_{.01}Al_{.05}Cr_{3.88}Fe_{2.89}Mg_{1.63}Mn_{.06}Ta_{.001})$	M=21.461	22.805
Bultfontein					
BD3096(1)	$(Ba_{.68}K_{.07}Sr_{.20}Ca_{.08}REE_{.03})$	A=1.06	$(Ti_{13.17}Zr_{.36}Al_{.11}Cr_{3.07}Fe_{3.42}Mg_{1.46}Nb_{.27})$ M=21.86	M=21.461	22.92
JJG360(1)	$(Ba_{.62}K_{.07}Sr_{.41}Ca_{.09})$	A=1.19	$(Ti_{11.63}Zr_{.87}Cr_{3.9}Fe_{2.87}Mg_{1.49})$	M=20.76	21.95
JJG360(2)	$(Ba_{.35}K_{.19}Sr_{.25}Ca_{.16})$	A=0.95	$(Ti_{12.83}Zr_{.41}Cr_{3.49}Fe_{2.42}Mg_{1.61})$	M=20.76	21.71
JJG360(3)	$(Ba_{.23}K_{.11}Sr_{.39}Ca_{.11})$	A=0.84	$(Ti_{12.32}Zr_{.61}V_{.14}Cr_{3.68}Fe_{2.44}Mg_{1.41}Mn_{.04})$	M=20.64	21.48
		MATHIASITE			
Kolonkwanen					
BD-2	$(K_{.66}Ba_{.10}Sr_{.15}Ca_{.22}Na_{.06})$	A=1.19	$(Ti_{13.18}Zr_{.62}Cr_{2.86}Fe_{2.28}Mg_{1.63}Nb_{.09})$	M=20.66	21.85
BD-4	$(K_{.67}Ba_{.09}Sr_{.15}Ca_{.22})$	A=1.13	$(Ti_{13.06}Zr_{.72}Cr_{2.98}Fe_{2.26}Mg_{1.56}Nb_{.09})$	M=20.67	21.80
Bultfontein					
3096(2)	$(K_{.45}Ba_{.21}Sr_{.19}Ca_{.17})$	A=1.02	$(Ti_{13.47}Zr_{.38}Cr_{2.96}Al_{.06}Fe_{3.27}Mg_{1.37})$	M=21.50	22.52
Jagersfontein					
JF26-3	$(K_{.46}Ba_{.13}Na_{.06}Ca_{.39}REE_{0.06})$	A=1.161	$(Ti_{12.98}Zr_{.66}Al_{.20}Cr_{3.72}Fe_{1.99}Mg_{1.77}Mn_{.04}Nb_{.06})$	M=21.42	22.581
JF41-1	$(K_{.35}Ba_{.13}Na_{.05}Ca_{.24}Sr_{.15}REE_{.16})$	A=1.08	$(Ti_{13.22}Zr_{.62}Al_{.19}Cr_{3.69}Fe_{1.60}Mg_{1.80}Mn_{.04})$	M=21.16	22.24
JF50-1	$(K_{.43}Ba_{.09}Na_{.01}Ca_{.32}Sr_{.13}REE_{.16})$	A=0.87	$(Ti_{12.83}Zr_{.65}Al_{.15}Cr_{3.88}Fe_{1.98}Mg_{1.77}Mn_{.04}Ta_{.016})$	M=21.316	22.186
Average of 29 nodules	$(K_{.45}Ba_{.11}Na_{.05}Ca_{.34}Sr_{.11}Pb_{.004}REE_{.18})$	A=1.24	$(Ti_{12.82}Zr_{.75}Al_{.22}Cr_{3.89}Fe_{1.91}Mg_{1.76}Mn_{.03}Nb_{.02}Ta_{.07})$	M=21.47	22.71
		LOVERINGITE			
Average	$(Ca_{.77}Na_{.02}Pb_{.007}K_{.01}Y_{.03}U_{.009}Th_{.017}REE_{.36})$	A=1.223	$(Ti_{12.50}Zr_{.61}V_{.24}Al_{.32}Cr_{.135}Fe_{4.3}Mg_{.59}Mn_{.04}Hf_{.02})$	M=19.97	21.193
		SENAITE			
	$(Pb_{0.77}Sr_{.04}Y_{.13}Ca_{.03}REE_{.04})$	A=1.01	$(Ti_{13.69}Fe_{6.0}Mn_{1.07}[V,Cr,Zr,Al]_{.24})$	M=21.00	21.01
		CRICHTONITE			
	$(Sr_{.71}Pb_{.06}Ca_{.02}Y_{.03}REE_{.10})$	A=0.92	$(Ti_{13.43}Fe_{6.71}Mn_{.69}[V,Cr.....]_{.17})$	M=21.00	21.92
		DAVIDITE			
	$(U_{.44}REE_{.90}Y_{.31}Ca_{.08}Pb_{.06})$	A=1.79	$(Ti_{12.07}Fe_{5.9}V_{.59}Cr_{.3}Mg_{.05}Al_{.08})$	M=19.08	20.87

Formulae derived on the basis of 38 oxygens from the compositions listed in Table 2.

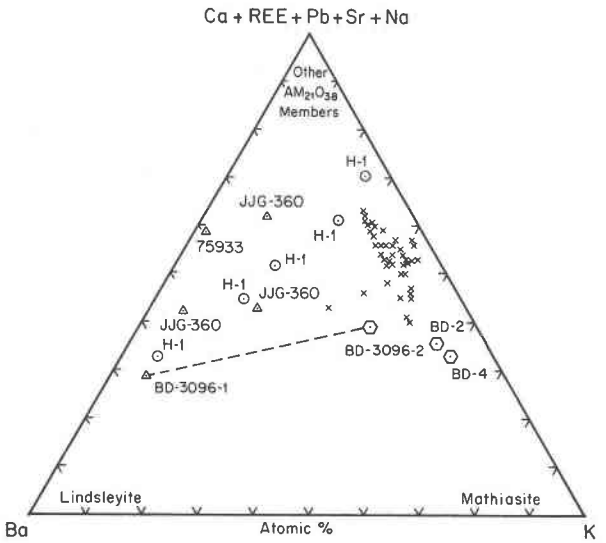

Fig. 2. Lindsleyite (circles and triangles) from De Beers (75933) and Bultfontein (JJG-360, BD-3096-1, this study; H-1, Jones *et al.*, 1982), and mathiasite (crosses, Jagersfontein; hexagons, BD-2 and BD-4, Kolonkwanen; and BD-3096-2 Bultfontein) expressed as a function of Ba, K, and other large cations. Lindsleyite and mathiasite coexist in BD-3096.

Large cations

Barium, the A position characteristic element in lindsleyite, is present in concentrations of 2.0 to 5.7 wt.% BaO. This represents a range of 0.234 to 0.679 cations filling the ideal 1.0 A-formula position. Other large cations present are Ca (0.085–0.156), Sr (0.196–0.254), Na (0–0.006), and REE (0.03–0.25), with Pb averaging 0.01, and K occupying 0.074–0.186 of the ideal 22 cations.

Potassium, the large cation in mathiasite, occupies a range of 0.352 to 0.665 cations in the A position. The Kolonkwanen mathiasite typically has 0.665 K, 0.055 Na, 0.102 Ba, 0.151 Sr and 0.216 Ca cations/38 oxygens. Average values for the 29 nodules from Jagersfontein have 0.448 K, 0.109 Ba, 0.337 Ca, 0.052 Na, 0.004 Pb, and 0.183 REE cations/38 oxygens. The Bultfontein mathiasite, BD 3096 (2) which also contains lindsleyite (Ba—0.68 cations in A), has 0.451 K and 0.208 Ba with the remaining cations totalling 0.395, for an overall sum of 1.054 cations in the ideal A = 1.0 position. The overall range of K_2O contents is 0.97–1.80 wt.%.

The extent to which Ba and K are present in other members of the $AM_{21}O_{38}$ crichtonite series cannot be evaluated. No data are reported for Ba and only landauite (Na-specific) has a K determination which is 0.29 wt.% K_2O, equivalent to 0.16 cations of the 1.08 present (Grey and Gatehouse, 1978). However, we can determine the extent of other members in solid solution in mathiasite and lindsleyite as illustrated in Figure 2. The range of other components (senaite, crichtonite, loveringite, davidite and landauite) is 29–67% for lindsleyite and 32–70% for mathiasite. Following the approach by Jones *et al.* (1982), Ba and Sr are combined, along with K and Na, and Ca + Pb + REE in Figure 3. There is a marked distribution of compositions from lindsleyite (Ba) + crichtonite (Sr) towards the (mathiasite + landauite)–(CaPbREE) sideline. This trend is defined by lindsleyites from Bultfontein and De Beers, together with mathiasites from Jagersfontein. The Kolonkwanen mathiasites, on the other hand, have K occupying 67% of the A position, an additional 20% of this position is made up by Ba + Sr, and the remainder, largely by Ca. The concentrations of Na are low in lindsleyite and mathiasite (0.18 wt.% Na_2O max) and the distribution of compositions in Figure 3, therefore, may be viewed as one that is dominated by Ba, Sr, and K. The sample containing very nearly the largest lindsleyite component JJG-360(1) with 5.4% BaO and 0.621 A cations also has the largest content of Sr (0.409 cations). The Sr (crichtonite) component is also present in mathiasite (≈15%), but is exceeded by Ca (loveringite) which is present in concentrations of 14–21%. Mathiasites from Kolonkwanen have, on average ≈33% loveringite and ≈11% crichtonite.

A consideration of the rare earth elements present (Table 2) shows that mathiasite, lindsleyite, and loveringite, along with davidite (REE + U specific), all have sizeable concentrations of REE. Loveringite and davidite are commonly metamict, but no evidence of metamictization is apparent in the new minerals and neither were U nor Th detected in electron microbeam analyses. Lindsleyite from De Beers (75933) is relatively enriched in REE with an average concentration of 2.25 wt.% (Table 1, column 3), and A = 0.245 cations. Fifteen of the 29 mathiasite nodules from Jagersfontein have been charac-

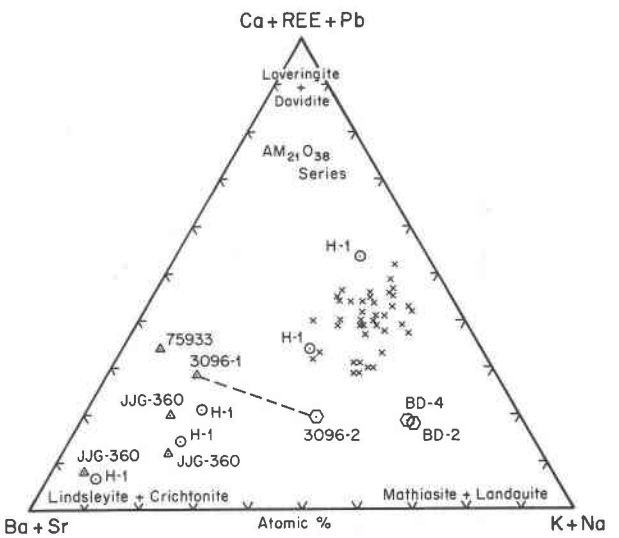

Fig. 3. A recombined expression of $AM_{21}O_{38}$ members illustrating the preferred trends of solid solution of (Ba + Sr) towards the join (K+Na) – (Ca+REE+Pb). Sample numbers and symbols are the same as those in Fig. 2.

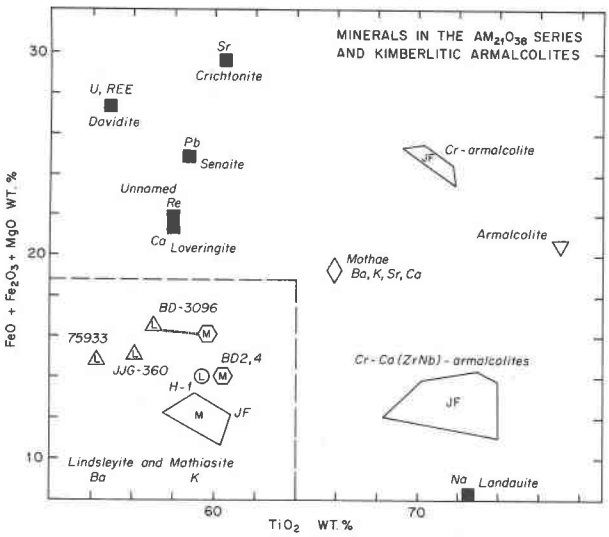

Fig. 4. A selected small cation plot illustrating the field for lindsleyite (L) and mathiasite (M) in comparison to other members of the $AM_{21}O_{38}$ series (Table 2); the unnamed rhenium (Re) member is from Sarp *et al.*, (1982). Armalcolites from the same suite of nodules as those containing mathiasite from Jagersfontein are shown as fields marked JF (Haggerty, submitted). The inverted triangle marked armalcolite is from Haggerty (1975), and the diamond symbol (Mothae) is either an armalcolite or a crichtonite member (Raber and Haggerty, 1979). The distribution of analyses lie in a TiO_2 "window" between ilmenite at lower TiO_2 contents, and rutile at higher values. Sample numbers and symbols are the same as those in Fig. 2.

terized for REE (Haggerty, submitted) and the average (Table 2, column 18) total concentration is 1.75 wt.% (A = 0.183 cations). These data, along with those for loveringite (Campbell and Kelly, 1978; Kelley *et al.*, 1979), and davidite (Hayton, 1960) are most unusual, insofar as the minerals are preferentially enriched in both the light and heavy rare earths and depleted in the middle lanthanides, normalized to chondritic abundances.

Small cations

The small cation M-position in the $AM_{21}O_{38}$ series for the new minerals is dominated by titanium (53–63 wt.% TiO_2), followed by Cr_2O_3 (13–18 wt.%), iron (FeO = 7–13 wt.%), zirconium (2–7 wt.%) and MgO (3–4 wt.%). Niobium concentrations range from 0.1 to 1.0 wt.% Nb_2O_5, vanadium is present at levels of 0.1 to 2.0 wt.%, with Al_2O_3 and MnO at concentrations of $\simeq$0.5 wt.% or less. Mathiasites from Kolonkwanen (BD2 and BD4) and Bultfontein (BD3096) are distinguished from those at Jagersfontein in that the latter have higher Cr_2O_3 ($\simeq$16 *vs.* $\simeq$12.5 wt.%) along with FeO ($\simeq$11 *vs.* $\simeq$8 wt.%); however FeO+MgO is relatively constant with an average value of 12.5 wt.%. Lindsleyites, on the other hand, have uniform concentrations of these elements and there are no distinguishing features in this mineral between the De Beers and Bultfontein varieties. The Fe/(Fe+Mg) ratios average 0.8 for lindsleyite, and 0.6 for mathiasite.

In respect to other members of the $AM_{21}O_{38}$ series, there are significant differences for most of the small cations. The relationship between $FeO+Fe_2O_3+MgO$ and TiO_2 is shown in Figure 4, along with data on kimberlitic armalcolites (Haggerty, submitted). Landauite is at the high TiO_2 end of the spectrum with low Fe+Mg values. The new minerals range from $\simeq$10 to $\simeq$18 wt.% FeO+MgO, whereas the remainder of the $AM_{21}O_{38}$ series have concentrations of 21–30 wt.% for virtually similar ranges in TiO_2. The new minerals may also be distinguished in Cr_2O_3 contents. Lindsleyite and mathiasite contain 12–18 wt.% Cr_2O_3, and the most similar of the other $AM_{21}O_{38}$ members is loveringite, which has an average Cr_2O_3 content of $\simeq$6 wt.% (range = 0.06–9.94 wt.%). Davidite has 1.2 wt.% Cr_2O_3 and the remaining members are at levels of less than 1.0 wt.%. Zirconium occurs in comparable concentrations in lindsleyite, mathiasite and loveringite and with average values of $\simeq$4 wt.% ZrO_2 (range = 1.2–6.1 wt.%). Manganese is present in concentrations of 2–4 wt.% MnO in senaite, crichtonite, and landauite in contrast to <0.25 wt.% for lindsleyite, mathiasite, davidite and loveringite.

The new minerals are distinguished, therefore, in the small cation position with large concentrations of chromium and with significant proportions of iron, magnesium, and zirconium. Among the remaining members of the series it is only loveringite that approaches the new minerals in respect to the small cation, M-formula unit.

Crystallography

Single-crystal fragments of representative analyzed specimens of each mineral were separated from polished sections, and X-ray powder diffraction patterns were obtained using a Gandolfi camera and Ni-filtered Cu$K\alpha$ radiation. The powder patterns are reported in Table 4. Single-crystal, X-ray precession photographs were taken of both minerals. The patterns observed were nearly identical for both minerals and indicated that the space group of both is $R\bar{3}$ or $R3$. The strongest reflections for lindsleyite are 2.13, 1.80, 1.59, and 1.44Å (all 100), and for mathiasite are 2.25(90), 2.14(100) and 1.44Å(100).

The crystal structures of crichtonite (Grey *et al.*, 1976) and senaite (Grey and Lloyd, 1976) are based upon a framework of close-packed oxygens preserving trigonal symmetry with 39 such anion sites in the rhombohedral cell. In this structure (space group $R\bar{3}$) there are eighteen octahedral cation sites (three nonequivalent sites, M_3, M_4, and M_5, each with a multiplicity of six) occupied primarily by Ti^{4+} and Fe^{3+}. There are two tetrahedral sites (one non-equivalent site, M_2, with a multiplicity of two) and one additional octahedral cation site (M_1, with a multiplicity of one). In addition, one of the 39 anion sites, M_0, is occupied by a large-radius cation so that it is coordinated by 12 oxygens. This gives a total of 22

Table 4. Powder X-ray diffraction patterns for mathiasite and lindsleyite

			Mathiasite		Lindsleyite	
h	k	$\ell_{(hex)}$	I	d	I	d
1	0	4	40	4.44		
1	1	3	50	4.14		
2	0	3	20	3.74		
1	2	0	60	3.39	30	3.37
2	0	4				
1	2	3	30	3.04	40	3.04
2	2	5				
3	0	0	80	2.99		
3	0	2	80	2.88	70	2.87
2	1	4	40	2.84	70	2.83
3	0	3	20	2.75	20	2.73
3	0	4	30	2.63	10	2.61
3	1	1	50	2.48	30	2.47
1	3	0				
2	2	3	40	2.43	30	2.39
4	0	0	90	2.25	40	2.24
3	1	4				
1	3	5	100	2.14	100	2.13
3	2	4	20	1.91	20	1.91
4	1	4	20	1.84	10	1.85
5	0	0	70	1.79	100	1.80
4	2	0	30	1.71	40	1.70
3	3	4	10	1.65		
5	1	0	10	1.61		
3	3	5	50	1.59	100	1.59
4	2	5	10	1.57		
3	3	6	10	1.55	20	1.55
4	2	6	10	1.52		
6	0	0	20	1.50	50	1.50
5	1	6	10	1.46		
6	0	4	100	1.44	100	1.44
5	2	0				
4	3	4	10	1.42		
4	3	5	10	1.41		
6	1	0	10	1.39		
6	1	1	10	1.37		

X-ray data by J.R. Smyth.

cations per 38 oxygens with a Z of 1 for the rhombohedral cell (Z = 3 for hexagonal cell, Table 5).

Discussion

Chemistry

A maximum of approximately 70% of the Ba (lindsleyite) component is present in the samples we report, and an almost equivalent value of 67% for the K component in the mathiasite member. These are, therefore, the dominant cations in the A characteristic position for the $AM_{21}O_{38}$ series. Dilution by other components is selective, and in part, predicted, insofar as Sr (crichtonite) replaces Ba in lindsleyite, and Ca (loveringite) is coupled with K in mathiasite. Na and Pb are present in minor proportions and the new minerals have characteristic REE patterns that are similar to those of davidite (U, REE) and loveringite, with enrichment in the light and heavy, and depletion of the middle REE. It is of interest to note that among other kimberlitic minerals perovskite is typically LREE–enriched and exhibits a systematic and strong depletion towards Lu, whereas zircon and garnet are LREE-depleted and strongly fractionate the heavy rare earths.

Lindsleyite and mathiasite are crystallographically established members of the $AM_{21}O_{38}$ crichtonite mineral series. However, we note that the large cation position is commonly in excess of 1.0 (Table 3) and this is consistently the case for the 29 mathiasite nodules from Jagersfontein. A number of tests have been undertaken to determine whether the difference can be attributed to analytical error or the presence of Ti^{3+} or Cr^{2+}. The results are negative, but another test shows that the formula is better suited to an anion basis of 17 oxygens which results in 10.0 cations. There are several possibilities which could account for this behavior: (1) the mathiasites from Jagersfontein are compositionally distinct, exhibiting large degrees of solubility of Ca and REE; (2) davidite (U, REE) has 2 cations in the A position rather than 1.0; and (3) all of the REE are included in the large cation position for the new minerals which may not be strictly correct (Campbell and Kelly, 1978), but would be consistent with the higher pressure origin of mathiasite and lindsleyite relative to other members of the crichtonite series.

In their detailed study of the REE distribution patterns of loveringite, Campbell and Kelly (1978) postulate lanthanide site preferences in the M_0 and M_1 sites, and conclude that depletion of the middle lanthanides is not the result of anomalous changes in the intercumulus liquid from which the loveringite grew, but rather a reflection of inter-site elemental exchange between M_0 and M_1. Whether this model is applicable to the new minerals described here cannot, as yet, be determined. Structural characterization of the Jagersfontein material is required along with an independent and more accurate determination of the REE. These data may shed information on the behavior of lanthanides in kimberlitic minerals and specifically those in high pressure environments.

Related minerals

Priderite has the formula $(K,Ba)(Ti,Fe)_8O_{16}$ and is an accessory mineral in diamond-bearing leucite-lamproites from the Kimberley region, Western Australia (Norrish, 1951; Jaques *et al.*, 1982). An unnamed mineral, $(K,Ba)_2$

Table 5. Cell parameters for crichtonite series minerals

Mineral	Lindsleyite	Mathiasite	Crichtonite	Senaite	Davidite	Loveringite	Landauite
Reference			1	2	3	4	5
Large Cation	Ba	K	Sr	Pb	U/REE	Ca	Na
Space Group	$R\bar{3}$	$R\bar{3}$	$R\bar{3}$	$R\bar{3}$	$R\bar{3}$	$R\bar{3}$	$R\bar{3}$
Rhombohedral Cell							
a (nm)	0.909	0.9098	0.9148	0.9172	0.9178	0.9117	0.9152
α (°)	69.6	69.34	69.078	69.020	68.80	69.07	68.99
V (nm^3)	0.6376	0.6364	0.6444	0.6489	0.6479	0.6378	0.6443
Hexagonal Cell							
a (nm)	1.037	1.035	1.0374	1.0393	1.037	1.0337	1.0366
c (nm)	2.052	2.058	2.0746	2.0811	2.087	2.0677	2.077
V (nm^3)	1.911	1.909	1.9336	1.9467	1.9436	1.9134	1.9328
Density (Calc)	4.63	4.60	4.54	4.59	4.44	4.59	4.46

1. *Grey et al. (1976)*
2. *Grey and Lloyd (1976)*
3. *Gatehouse et al. (1979)*
4. *Gatehouse et al. (1978)*
5. *Grey and Gatehouse (1978)*

Lindsleyite and mathiasite by J.R. Smyth.

$(Ti,Fe)_6O_{13}$, is reported from the same district in association with priderite and perovskite (Bagshaw *et al.*, 1977). Both priderite and the unnamed mineral lack Cr_2O_3 as an essential constituent, but another mineral, $K(Cr,Ti,Fe,Mg)_{11}O_{17}$, from the Yimeng mountain, Shandong, kimberlite in China (Jianxiong, 1980; pers. comm. to SEH, 1982), bears a compositional similarity to mathiasite. A priderite-related mineral, having K and Ba as major components, is also reported by Jones *et el.*, (1982) in one of their veined metasomites from Bultfontein.

Loveringite, senaite, crichtonite, and landauite occur as accessory minerals in mafic and alkali complexes (Campbell and Kelly, 1978; Grey *et al.*, 1976), but davidite has a wide distribution that ranges from metamorphic rocks to hydrothermal associations (Butler and Hall, 1960). Loveringite is most similar in large and small cations to the new minerals described here, and this is consistent with the high Ca affinity of kimberlites. An unnamed Re member of the crichtonite series is reported by Sarp *et al.* (1981), and phases bearing a close compositional resemblance to the M-formula position are present in the Bushveld complex (Cameron, 1978). The low Cr_2O_3 but K, Ca, Sr and Ba-bearing mineral that forms at the reaction interfaces of zircon and rutile (Raber and Haggerty, 1979) from the Mothae kimberlite may also be a member of the crichtonite series.

Genesis

Lindsleyite and mathiasite are dominated by highly refractory elements (Cr, Ti, Zr, REE) and for the most part these elements are also silicate-incompatible. Among the commonly associated minerals that are present are Nb- and Cr-bearing rutiles and ilmenites together with the only well documented mineral "sinks" for mantle volatiles, namely phlogopite and K-richterite. The new mineral assemblage is remarkably similar to the MARID (mica, amphibole, rutile, ilmenite, diopside—but also zircon) suite of kimberlite nodules which Dawson and Smith (1977) and Jones *et al.* (1982) interpret as a mantle pegmatite facies perhaps related to proto-kimberlite formation. In the case of peridotites containing the new mineral assemblage, Erlank and Rickard (1977), and Shimizu and Allegre (1977) provide sound arguments for upper mantle metasomatism, while Sr and Nd isotopic data indicate that the metasomatic event(s) predated, and are not related to kimberlite emplacement or formation (Erlank and Shimizu, 1977; Erlank *et al.*, 1982). Their evidence hinges in part on the association of K-richterite, phlogopite, diopside, lindsleyite and mathiasite in both veined and unveined peridotites. This suggests that a coherent sequence from lherzolite or harzburgite, to lherzolite or harzburgite + phlogopite + K-richterite + the new minerals will develop in low aluminum environments (K-richterite is not stable in the presence of garnet and Al-rich spinel) if K and Ba are abundant in the metasomatizing fluids. In the model presented by Jones *et al.* (1982), the hybridization of Cr-rich wall-rocks is invoked, distinguishing the new mineral metasomites from the MARID suite which has only ilmenite present and hence, reflects an absence of Cr-wall contaminants. In addition, the MARID suite lacks olivine, in contrast to the metasomatized peridotites which also contain lindsleyite and mathiasite. The precise relationship, if any, between the two nodule suites requires further study.

Ca–Cr(ZrNb) armalcolite is present in one of our Bultfontein nodules (Fig. 5), occurs in association with Nb–Cr-rutile in the Jagersfontein megacrysts, and is also present (incorrectly identified as phase H-1, *i.e.*, linds-

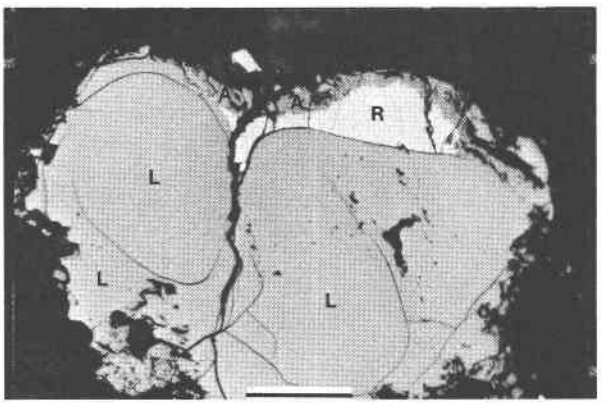

Fig. 5. A reflected light oil-immersion photomicrograph of lindsleyite (L) with characteristic curvilinear cracks, mantled successively by rutile (R), which contains lamellar ilmenite, and armalcolite (A). The assemblage is surrounded by chrome diopside. Sample JJG-360, Bultfontein. Scale bar = 0.1mm.

leyite) in one of the lindsleyite-bearing metasomites described by Jones *et al.* (1982). High pressure (5–20 kbar) studies on Cr- and Zr-doped armalcolites (Lindsley *et al.*, 1974; Kesson and Lindsley, 1975; Friel *et al.*, 1977) show a *P–T* dependency on lower thermal stability limits, and although the effect of Nb remains unknown, the limits of stability are ≈20 kbar for armalcolite low in MgO and Cr_2O_3. Erlank and Kushiro (1970) and Kushiro and Erlank (1970) have demonstrated that K-richterite, under H_2O saturated conditions, is stable to at least 30 kbar at 1100°C, and to 1000°C at 24 kbar in the presence of diopside. We suggest, therefore, that lindsleyite and mathiasite are probably stable at P = 20–30 kbar and 1000–1100°C which would lie in the range of the shield geotherm at depths of 75–100 km.

In the models presented it is implied that the composition of the fluid or the contaminants require rather special conditions or circumstances for the formation of lindsleyite and mathiasite. These new minerals and armalcolite occupy a TiO_2, Cr_2O_3, and Fe–Mg compositional "window" between ilmenite and rutile (Fig. 4) which may be *P–T* dependant for stabilization. Ilmenite has less TiO_2 than lindsleyite or mathiasite, and rutile has greater concentrations of TiO_2 than armalcolite.

Applications

Lindsleyite and mathiasite constitute potentially important new mineral, high pressure reservoirs, for refractory and large-ion-lithophile elements in the Earth's upper mantle. These phases may, therefore, be fundamental to an understanding of the dynamics of fluid movements, and metasomatizing compositions in the region of the lower continental lithosphere and upper asthenosphere. We consider that the new minerals may be relatively common but generally overlooked because of their similarity in optical properties to ilmenite and rutile.

The new minerals, and members of the crichtonite series, may have a direct application to SYNROC-type (Ringwood, 1978) repositories for the disposal of radioactive nuclear waste products, given their structural flexibility in hosting large and small radii cations that include Ti, Zr, Cr, alkalies, U, Th, the rare earths, and because the series is highly refractory.

Acknowledgments

We acknowledge the cooperation of De Beers Consolidated Mines and J. B. Hawthorne in particular for his support in granting permission to sample the sites quoted in this collaborative study. SEH wishes to acknowledge the National Science Foundation for partial support under grants EAR-78-02541 and EAR-76-23787, and extends his thanks to De Beers and the Anglo American Corporation for hosting the "Opaque View of the Mantle" short course in 1977 which resulted in the identification of a single mathiasite nodule from Jagersfontein (the remaining samples discussed here were collected in 1980). AJE and RSR thank the University of Cape Town and the CSIR for financial support, and J. J. Gurney and J. B. Dawson for their assistance in collecting samples for this study. We are indebted to C. J. Stanley of the British Museum (Natural History) who undertook the reflectivity measurements and provided access to SEH for hardness determinations. A critical review was provided by P. B. Moore of the University of Chicago.

References

Ahrens, L. H., Dawson, J. B., Duncan, A. R. and Erlank, A. J. (1975) Proceedings 1st International Kimberlite Conference. Physics and Chemistry of the Earth, 9.

Albee, A. L. and Ray, L. (1970) Correction factors for electron probe microanalysis of silicates, oxides, carbonates, phosphates, and sulfates. Analytical Chemistry, 42, 1408–1414.

Åmli, R. and Griffin, W. L. (1975) Microprobe analysis of REE minerals using empirical correction factors. American Mineralogist, 60, 599–606.

Bagshaw, A. N., Doran, B. H., White, A. H., and Willis, A. C. (1977) Crystal structure of a natural potassium-barium hexatitanate isostructural with $K_2Ti_6O_{13}$. Australian Journal of Chemistry, 30, 1195–1200.

Bence, A. E. and Albee, A. L. (1968) Empirical correction factors for the electron microanalysis of silicates and oxides. Journal of Geology, 76, 382–403.

Boyd, F. R. and Meyer, H. O. A. (1979a) Kimberlites, diatremes, and diamonds: Their geology, petrology, and geochemistry. Proceedings 2nd International Kimberlite Conference. American Geophysical Union, Washington, D.C.

Boyd, F. R. and Meyer, H. O. A. (1979b) The mantle sample: Inclusions in kimberlites and other volcanics. Proceedings 2nd International Kimberlite Conference. American Geophysical Union, Washington, D.C.

Butler, J. R. and Hall, R. (1960) Chemical characteristics of davidite. Economic Geology, 55, 1541–1550.

Cabri, L. J., Criddle, A. J., LaFlamme, J. H. G., Bearne, G. S., and Harris, D. C. (1981) Mineralogical study of complex Pt–Fe nuggets from Ethiopia. Bulletin de Minéralogie, 104, 508–525.

Cameron, E. M. (1978) An unusual titanium-rich oxide mineral from the Eastern Bushveld Complex. American Mineralogist, 63, 37–39.

Campbell, I. H. and Kelly, P. R. (1978) The geochemistry of loveringite, a uranium-rare-earth-bearing accessory phase

from the Jimberlana intrusion of Western Australia. Mineralogical Magazine, 42, 187–197.

Criddle, A. J. (1980) Editorial policy for the second issue of the IMA/COM quantitative data file. Canadian Mineralogist, 18, 553–558.

Dawson, J. B. and Smith, J. V. (1977) The MARID (mica–amphibole–rutile–ilmenite–diopside) suite of xenoliths in kimberlite. Geochemica et Cosmochimica Acta, 44, 309–323.

Drake, M. J. and Weill, D. F. (1972) New rare earth elements standards for electron microprobe analysis. Chemical Geology, 10, 179–181.

Erlank, A. J. and Kushiro, I. (1970) Potassium contents of synthetic pyroxenes at high temperatures and pressures. Carnegie Institution of Washington Year Book, 68, 233–236.

Erlank, A. J. and Rickard, R. S. (1977) Potassic richterite bearing peridotites from kimberlite and the evidence they provide for upper mantle metasomatism. (abstr.) Second International Kimberlite Conference, Santa Fe, New Mexico.

Erlank, A. J. and Shimizu, N. (1977) Strontium and strontium isotope distributions in some kimberlite nodules and minerals. (abstr.) 2nd International Kimberlite Conference, Sante Fe, New Mexico.

Erlank, A. J., Allsopp, H. L., Hawkesworth, C. J., and Menzies, M. A. (1982) Chemical and isotopic characterization of upper mantle metasomatism in peridotite nodules from the Bultfontein Kimberlite. Terra Cognita, 2, 261–263.

Friel, J. J., Harker, R. I., Ulmer, G. C. (1977) Armalcolite stability as a function of pressure and oxygen fugacity. Geochimica et Cosmochimica Acta, 41, 403–410.

Gatehouse, B. M., Grey, I. E., Campbell, I. H., and Kelly, P. (1978) The crystal structure of loveringite—a new member of the crichtonite group. American Mineralogist, 63, 28–36.

Gatehouse, B. M., Grey, I. E., and Kelly, P. (1979) The crystal structure of davidite from Arizona. American Mineralogist, 64, 1010–1017.

Grey, I. E. and Lloyd, D. J. (1976) The crystal structure of senaite. Acta Crystallographica B32, 1509–1513.

Grey, I. E., Lloyd, D. J., and White, Jr. J. S. (1976) The crystal structure of crichtonite and its relationship to senaite. American Mineralogist, 61, 1203–1212.

Grey, I. E. and Gatehouse, B. M. (1978) The crystal structure of landauite, $Na\,[MnZn_2(Ti,Fe)_6Ti_{12}]O_{38}$. Canadian Mineralogist, 16, 63–68.

Haggerty, S. E. (1975) The chemistry and genesis of opaque minerals in kimberlites. Physics and Chemistry of the Earth, 9, 295–307.

Haggerty, S. E. (1979) The Jagersfontein kimberlite, South Africa: An emporium of exotic mineral reactions from the upper mantle. (abstr.) Geological Society of America Abstracts with Programs, 11, 437.

Haggerty, S. E. (1982) Complex titanate compounds (MO_2, M_2O_3, M_3O_5, M_4O_7, $M_{22}O_{38}$) in Kimberlites: Mineral repositories for and the partitioning of LIL elements. (abstr.) Terra Cognita, 2, 225.

Harte, B. and Gurney, J. J. (1982) Compositional and textural features of peridotite nodules from the Jagersfontein Kimberlite pipe, South Africa. Terra Cognita, 2, 256–257.

Hayton, J. D. (1960) The constitution of davidite. Economic Geology, 55, 1030–1038.

Jaques, A. J., Gregory, G. P., Lewis, J. D., and Ferguson, J. (1982) The ultrapotassic rocks of the West Kimberley region, Western Australia, a new class of diamondiferous kimberlite. Terra Cognita, 2, 251–252.

Jianziong, Zhou. (1980) Microanalysis techniques of minerals and their geological application. [in Chinese] Geological Review, 6, 547–551.

Johnston, J. L. (1973) Petrology and geochemistry of ultramafic xenoliths from the Jagersfontein Mine. OFS. South Africa. (abst.) First International Kimberlite Conference, Cape Town, 181–183.

Jones, A. P., Smith, J. V., and Dawson, J. B. (1982) Mantle metasomatism in 14 veined peridotites from the Bultfontein Mine, South Africa. Journal of Geology, 90, 435–453.

Kelly, P. R., Campbell, I. H., Grey, I. E., and Gatehouse, B. M. (1979) Additional data on loveringite (Ca,REE) (Ti, Fe, $Cr)_{21}O_{38}$ and mohsite discredited. Canadian Mineralogist, 17, 635–638.

Kesson, S. E. and Lindsley, D. H. (1975) The effects of Al^{3+}, Cr^{3+}, and Ti^{3+} on the stability of armalcolite. Proceedings Lunar Science Conference, 6th, Supp. 6, Geochimica et Cosmochimica Acta, 1, 911–920.

Kushiro, I., and Erlank, A. J. (1970) Stability of potassic richterite. Carnegie Institution of Washington Year Book, 68, 231–233.

Lindsley, D. J., Kesson, S. E., Hartzman, M. J., and Cushman, M. K. (1974) The stability of armalcolite: experimental studies in the system MgO–Fe–Ti–O. Proceedings Lunar Science Conference 5th, Supp. 5, Geochimica et Cosmochimica Acta, 1, 521–534.

MacGregor, I. D. and Carter, J. L. (1970) The chemistry of clinopyroxenes and garnets of eclogite and peridotite xenoliths from the Roberts Victor Mine, South Africa. Physics of the Earth and Planetary Interiors, 3, 391–397.

Norrish, K. (1951) Priderite, a new mineral from the leucite-lamproites of the West Kimberley area, Western Australia. Mineralogical Magazine, 29, 406–501.

Raber, E. and Haggerty, S. E. (1979) Zircon-Oxide reactions in Kimberlites. In F. R. Boyd and H. O. A. Meyer, Eds., Kimberlites, diatremes and diamonds: Their geology, petrology and geochemistry, p. 229–240. Proceedings 2nd International Kimberlite Conference. American Geophysical Union, Washington, D.C.

Ringwood, A. E. (1978) Safe disposal of high-level nuclear reactor wastes: A new strategy. Australian National University Press, p. 64.

Rouse, R. C. and Peacor, D. R. (1968) The relationship between senaite, magnetoplumbite and davidite. American Mineralogist, 53, 869–879.

Sarp, H., Bertrand, J., Deferne, J., and Liebich, B. W. (1981) A complex rhenium-rich titanium and iron oxide of the crichtonite-senaite group. Neus Jahrbach für Mineralogie Monatshefte, 10, 433–442.

Shimizu, N. and Allegre, C. J. (1977) Geochemistry of transition elements in garnet lherzolite nodules in kimberlites. (abstr.) 2nd International Kimberlite Conference, Santa Fe, New Mexico.

Smyth, J. R., Erlank, A. J., and Rickard, R. S. (1978) A new Ba–Sr–Cr–Fe titanate mineral from a kimberlite nodule. (abstr.) EOS. American Geophysical Union, 59, 394.

Manuscript received, August 27, 1982;
accepted for publication, January 10, 1983.